ELSEVIER

Aerobic oxidation of alcohols by organically modified ruthenium hydroxyapatite

Z. Opre, D. Ferri, F. Krumeich, T. Mallat, A. Baiker *

Institute for Chemical and Bioengineering, ETH Zurich, Hönggerberg, HCI, CH-8093 Zurich, Switzerland

Abstract

The activity of ruthenium-hydroxyapatite (RuHAp) in the oxidation of benzyl alcohol with molecular oxygen was more than tripled by the incorporation of Ru into organically modified HAp and no detectable product beside benzaldehyde was formed. The effective modifiers prolinol, proline, benzoic acid, and hexanoic acid have functional groups that can form strong hydrogen bonds with the surface OH and phosphate groups of HAp. On the basis of catalytic, DRIFT, SEM, STEM-EDX, ICP-OES, and BET measurements, we assume that the major reason for the activity enhancement is the higher intrinsic activity of Ru species due to their different location and coordination in organically modified HAp. It is very probable that incorporation of Ru is not an ion-exchange process, but rather an adsorption process controlled by the polar organic compounds. Interestingly, during this process the modifiers leach out and thus do not disturb the catalytic oxidation of alcohols. The slope of the Hammett plot of p-substituted benzyl alcohols indicates that β-hydride elimination from the alcoholate intermediate is the rate-determining step under kinetically controlled reaction conditions. The catalysts are reusable with no sign of Ru leaching.

1. Introduction

There is a growing need for "green" technologies in the synthesis of fine chemicals and pharmaceutical intermediates. For catalytic oxidation, an attractive approach is the use of a solid, recyclable catalyst and molecular oxygen as the only oxidant, that is, without any sacrificial reductant or other additive. Another important target is to achieve the highest possible yield and thus minimize the additional costs of separation and waste removal that may be a critical factor in a small-scale synthesis [1–6].

There are only a few heterogeneous catalysts that afford the quantitative transformation of primary alcohols to aldehydes, and the production rates characterized by the average turnover frequency (TOF) at high yields are frequently insufficient for practical application [7–14]. Supported Pt and Pd catalysts are more active, but, with a few exceptions, further oxidation of the

aldehyde to carboxylic acid is significant [2,15–17]. In aqueous alkaline medium, gold nanoparticles are highly active under very mild conditions and provide the corresponding carboxylic acid in excellent yield [18–20]. In the absence of a base co-catalyst, the aldehyde is the major product, but below 373 K commonly applied in the synthesis of fine chemicals, the reaction rates are moderate [21]. Recently, outstanding rates (initial TOF up to 86,500 h^{-1}) have been achieved under solvent-free conditions with supported Au and Pd–Au catalysts [22–24]; however, the required high reaction temperature (433 K) limits the use of these catalysts for the synthesis of complex, thermo-labile compounds typical in fine chemistry, and the selectivities at this elevated temperature are poor, only around 60%.

Hydroxyapatite [$Ca_{10}(PO_4)_6(OH)_2$, HAp]-based materials have attracted increasing interest as solid, recyclable catalysts. Sebti et al. have developed a wide spectrum of heterogeneous catalysts based on the apatite structure to catalyze several organic reactions [25–27], including Knoevenagel condensation [28,29], Friedel–Crafts alkylation [30], and Michael addition [31]. Apatites are also effective in the conversion

of alcohols to aldehydes. Calcium phosphate–vanadate apatite catalyzes the aerobic oxidation of propargylic alcohols [32], whereas Pd nanoparticles supported on HAp and ionic Ru incorporated into the HAp matrix (RuHAp) are effective in the oxidation of various primary and secondary alcohols [17,33]. RuHAp is also a good catalyst for the mild racemization of chiral secondary alcohols [34].

A disadvantage of high Ru loading (17 wt%) in the original RuHAp catalyst [33] is that Ru ions incorporate deeply inside the microporous channels of HAp, resulting in poor accessibility of the active sites and rather low alcohol oxidation activity (TOF 0.6–6 h^{-1}). Enhancement of the redox activity of the catalyst requires reduction of the total amount of Ru ions and controlling their location in HAp [34,35]. The preferential location of the isolated Ru ions close to the surface of HAp particles could be achieved by using promoting metal ions (Co^{2+} and Pb^{2+}), which occupy the "hidden" sites inside the narrow channels, and by applying short contact times during incorporation of Ru [35]. These modifications enhance the activity in alcohol oxidation by more than an order of magnitude and increase the selectivity to the corresponding carbonyl compounds to 100% [36]. In situ EXAFS analysis during benzyl alcohol oxidation and a detailed kinetic study [36] revealed that (i) the probable active sites are dihydroxo ruthenium species, (ii) the oxidative dehydrogenation reaction obeys the Mars–van Krevelen mechanism, and (iii) the reduced hydrido-ruthenium species is inactive in alcohol dehydrogenation without reoxidation by molecular oxygen. Depending on the actual oxygen concentration at the catalyst surface, the rate-limiting step is either the reoxidation of the ruthenium hydride species or the β-hydride elimination step from the alcoholate intermediate.

Another approach to enhancing the activity of RuHAp while maintaining its excellent selectivity is organic modification. Surface modification of HAp with alkyl phosphates [37–40], dodecyl alcohol [41], alkenoic acids [42], and amino acids [43,44], and the effect of amino acids on the mineralization of HAp [45–48] have already been reported. Here we report the effect of organic modification on the catalytic properties of RuHAp in the oxidation of benzylic alcohols and 2-octanol (Scheme 1), used as model reactions for the oxidation of aromatic and aliphatic alcohols. The structure of the new catalysts and the mechanism of the reaction have been investigated using various techniques.
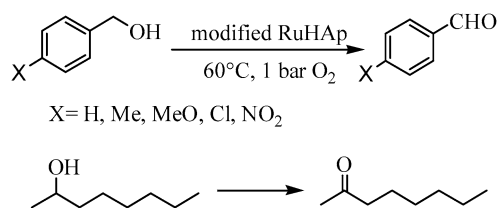
Scheme 1. Oxidation of benzylic alcohols and 2-octanol with oxygen on organically modified RuHAp. No other product beside the carbonyl compounds could be detected.

2. Experimental

2.1. Materials

Starting materials for catalyst preparation were RuCl$_3$ hydrate (36% Ru, 99.9%, ABCR), aqueous ammonia solution (ca. 25% NH$_3$, Merck), (NH$_4$)$_2$HPO$_4$ (98%, ABCR), Ca(NO$_3$)$_2$·4H$_2$O (99%, Strem Chemicals), hexanoic acid (>99.5%, Aldrich), 2-ethylhexyl-phosphate (VWR), proline (>99.5%; Fluka), prolinol (2-(hydroxymethyl)pyrrolidine) (>98%, Lancaster), and benzoic acid (>99.5%; Aldrich). Benzyl alcohol (>99%; Fluka), 4-nitrobenzyl alcohol (99%, Acros), 4-chlorobenzyl alcohol (99%, Acros), 4-methoxybenzyl alcohol (>98%, Acros), 4-methylbenzyl alcohol (99%, ABCR), 2-octanol (99.5%; Fluka), toluene (Baker) and mesitylene (98%, Acros) were used as received.

2.2. Catalyst preparation

Two different methods were found to be useful for the preparation of organically modified HAp. In method I, stoichiometric HAp was first synthesized by a wet chemical method using Ca(NO$_3$)·4H$_2$O and (NH$_4$)$_2$HPO$_4$, and then calcined at 773 K for 3 h [49]. Then surface modification of HAp with hexanoic acid (resulting in "HAp-HAcid") and 2-ethylhexyl-phosphate (resulting in "HAp-Phos") was carried out as follows. A 1-g HAp sample was stirred at reflux temperature for 5 h in 60 mL of 1.36 M solution of hexanoic acid in hexane or in 60 mL of 0.01 M 2-ethylhexyl-phosphate solution in a 2:1 acetone–water mixture. The modified apatite HAp-HAcid and HAp-Phos were filtered off, washed with hexane or acetone, respectively, and dried in vacuum for 24 h at room temperature.

In method II, the organic modifier proline, prolinol, or benzoic acid was added during the preparation of HAp using a molar ratio of Ca(NO$_3$)$_2$:(NH$_4$)$_2$HPO$_4$:organic modifier of 1:0.6:0.31. The (NH$_4$)$_2$HPO$_4$ solution was added to the Ca(NO$_3$)$_2$ solution containing the organic modifier. In the case of the poorly soluble benzoic acid, the solution was refluxed. Otherwise, the preparation followed the procedure described by Sugiyama et al. [49]. The materials HAp-proline, HAp-prolinol, and HAp-BAcid (HAp-benzoic acid) were dried overnight at 363 K. Incorporation of Ru was carried out by shaking 1.0 g of organically modified HAp with 75 mL of a 6.7 mM aqueous RuCl$_3$ solution at room temperature for 10 min [35]. The catalyst was filtered off, washed with deionized water, and dried at room temperature for 6 h in vacuum.

2.3. Characterization techniques

The BET surface area and pore size distribution were determined by N$_2$ adsorption–desorption at 77 K using a Micromeritics ASAP 2010 instrument. Before measurement, the samples were degassed in vacuum at 333 K. Powder X-ray diffraction (XRD) analysis was carried out on a Siemens D5000 powder X-ray diffractometer using the Cu-K$_\alpha$ radiation in the step-scanning mode between 20° and 80° (2θ), with a step size of 0.01° and 2 s/step. Diffuse reflectance infrared (DRIFT)

spectra were collected with a Bruker Optics Equinox-55 by co-adding 100 scans at 4-cm^{-1} resolution. The instrument was equipped with a HVC-DRP2 reaction chamber (Harrick) and a liquid N$_2$-cooled MCT detector. Samples were diluted with KBr, and reference spectra of KBr were acquired at room temperature. The Ca, P, and Ru contents in the catalyst samples were determined by inductively coupled plasma optical emission spectroscopy (ICP-OES).

Scanning electron microscopy (SEM) investigations of the as-synthesized samples were performed on a Gemini 1530 (Zeiss) at low voltage ($U = 1$ keV; field emission gun). For scanning transmission electron microscopy (STEM), the samples were suspended in ethanol, and some droplets were deposited on a holey carbon foil supported on a copper grid. The investigation was performed on a field emission transmission electron microscope (Tecnai 30F, FEI, with a SuperTwin lens with $C_s = 1.2$ mm), operated at 300 kV. STEM images were recorded with a high-angle annular dark field (HAADF) detector, using almost exclusively incoherently scattered electrons (Rutherford scattering) to obtain images with atomic number (Z) contrast [50]. An energy-dispersive X-ray (EDX) spectrometer attached to the Tecnai F30 enables performance of elemental analyses on selected spots (diameter 3–5 nm) in the HAADF-STEM images [51].

2.4. Alcohol oxidation

The catalytic tests were performed with pure O$_2$ at 1 bar and 333 K using a solution of 1 mmol alcohol in toluene or mesitylene and 10–60 mg of catalyst. After reaction, the catalyst was filtered off and washed carefully with 2-propanol. The selectivity and conversion were determined by gas chromatography analysis (Thermo Quest Trace 2000, equipped with an HP-FFAP capillary column and a flame ionization detector), and the products were identified by authentic samples.

The role of oxygen transfer into the liquid phase and to the catalyst surface and that of adsorption of water co-product on RuHAp was discussed in a previous study [36]. The reaction rate was characterized by the turnover frequency (TOF), {mol(alcohol)/(mol(Ru) h)}, calculated at full conversion (TOF$_{av}$) and at 5% conversion (TOF$_0$), if not otherwise stated. Note that the reported TOFs represent conservative estimates because they are based on the determination of the number of Ru sites by ICP-OES, not on the real number of accessible sites.

3. Results

3.1. Catalyst characterization

The XRD patterns of the modified HAp and RuHAp samples revealed only the characteristic peaks of HAp. This observation is in agreement with those of previous studies on RuHAp [35,36]. The crystallinity was not influenced by the surface treatment of HAp according to method I, but synthesis of HAp in the presence of organic modifier (method II) resulted in considerable line-broadening, indicating decreasing crystallite size

Table 1

Characterization of (organically modified) HAp and RuHAp materials by ICP-OES analysis and BET measurement

	Organic modification method	Ca/P	(Ca + Ru)/P	Ru (mmol/g)	BET (m^2/g)
HAp	–	1.67	–	–	60
RuHAp	–	1.60	1.66	0.37	65
HAp-Phos	I	1.52	–	–	55
RuHAp-Phos	I	1.59	1.64	0.28	73
RuHAp-HAcid	I	1.58	1.63	0.28	77
HAp-BAcid	II	1.61	–	–	51
RuHAp-BAcid	II	1.61	1.66	0.31	82
HAp-proline	II	1.52	–	–	75
RuHAp-proline	II	1.52	1.59	0.35	107
HAp-prolinol	II	1.63	–	–	77
RuHAp-prolinol	II	1.63	1.68	0.34	100

of the HAp phase. It is known from the literature that amino acids have an inhibitory effect on the crystal growth of HAp, possibly through adsorption onto the active growth sites of the HAp crystal surface [44,45,48]. Introducing Ru barely influenced the crystallinity, because the short contact time between HAp and the RuCl$_3$ solution prevented a considerable restructuring, as described previously [35].

The Ca/P and (Ca + Ru)/P ratios and the Ru content of the samples were measured by ICP-OES (Table 1). The Ca/P ratio in HAp corresponded to the theoretical value of stoichiometric HAp (1.67). The Ca/P ratio of RuHAp decreased compared with that of pure Hap, and the (Ca + Ru)/P ratio was 1.66, in agreement with the partial replacement of Ca^{2+} ions by cationic Ru species. In contrast, in the organically modified HAp samples (HAp-Phos, HAp-BAcid, HAp-proline, HAp-prolinol), the Ca/P ratios were significantly lower than 1.67, revealing the nonstoichiometric nature of these materials. Moreover, introducing Ru into the organically modified HAp samples did not reduce the Ca/P ratio, suggesting that incorporating Ru into the apatite lattice is not an ion-exchange process.

The BET surface areas of organically modified RuHAp samples were 20–80% higher than those of unmodified RuHAp (Table 1). Another interesting observation is that incorporation of Ru changed the surface area of unmodified Hap only marginally, but produced an increase of around 30 m^2/g in the case of organically modified HAp samples. The latter effect may be attributed to the simultaneous dissolution (leaching) of the organic modifier. A similar phenomenon was observed previously with HAp modified by alkyl phosphate and hexanoic acid, where removal of the modifiers by outgassing at 473 K provided materials of higher surface area [37,42]. Evidence of leaching of the organic modifier during Ru incorporation by IR spectroscopy is given below.

The morphology of the catalysts was investigated by SEM; some representative micrographs are collected in Fig. 1. HAp prepared in the absence of organic modifier formed dense plate-like aggregates (Fig. 1A). No obvious morphological difference could be observed between unmodified HAp and surface-modified HAp (see method I), but HAp modified during its synthesis (according to method II) showed a decrease in the
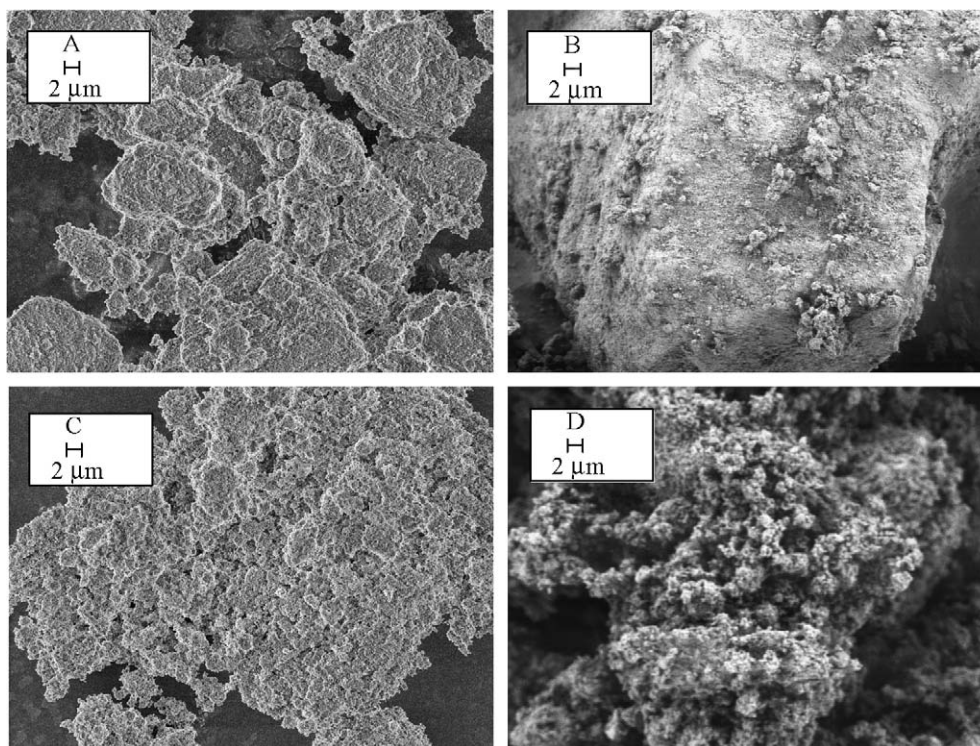
Fig. 1. SEM images of HAp (A), RuHAp (B), HAp-BAcid (C), and RuHAp-BAcid (D).
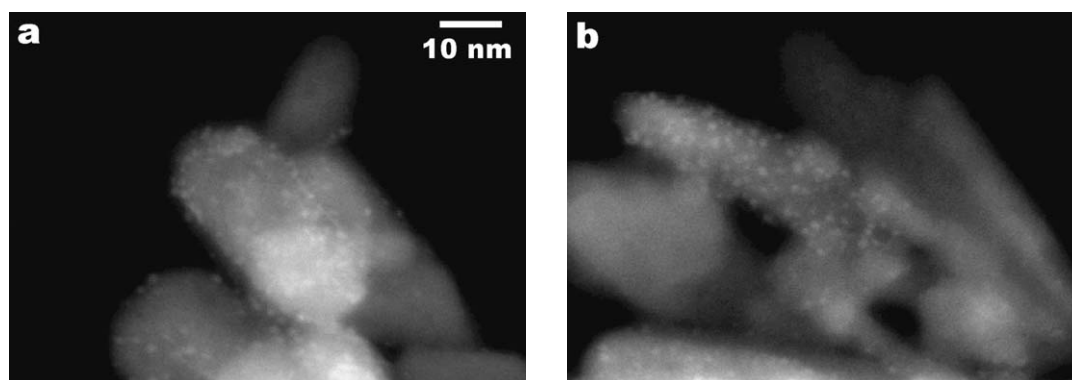

Fig. 2. HAADF-STEM images of (a) RuHAp and (b) RuHAp-BAcid. In both cases, some of the HAp crystals are covered by Ru particles (bright spots).

average size of the fragments of aggregates, and the surface appeared smoother compared to HAp (Fig. 1C). After incorporation of Ru into unmodified Hap, the structure became quite compact (Fig. 1B). On the other hand, the structure of RuHAp samples modified organically according to method II were fluffy, as illustrated by the micrograph of RuHAp-BAcid (Fig. 1D). The morphological changes revealed by SEM are in good agreement with the increased surface area of RuHAp-proline, RuHAp-prolinol, and RuHAp-BAcid catalysts (Table 1) and provide further evidence against the simple exchange of Ca ions by Ru ions as the ruling mechanism.

HAADF-STEM images of the RuHAp and RuHAp-BAcid samples revealed some of the crystals coated with bright dots (Fig. 2). Because Ru is the strongest scatterer in this system (i.e., has the highest atomic number), the sites in which Ru is located appear with the brightest contrast. Therefore, the bright

dots correspond to Ru "particles" (possibly aggregates of Ru^{3+} species), which are about 1 nm in diameter. The micrographs reveal the inhomogeneous distribution of Ru on the HAp crystals. In both samples, the Ru loading varies from crystal to crystal, and even crystals without Ru are present (see, e.g., the crystal on the left side of Fig. 2b). Interestingly, the Ru species appeared on the crystal surface, and no significant difference could be observed between the Ru distributions in conventionally prepared and organically modified RuHAp samples. We note that reduction of Ru^{3+} in the electron beam to metallic Ru and also some restructuring of Ru during the measurement cannot be ruled out.

The unexpected inhomogeneous distribution of Ru in the apatite matrix was confirmed by EDXS spot analyses (Fig. 3). When the spot was set on areas containing bright dots, peaks characteristic of Ru (i.e., K peaks at ~19.2 and ~22 keV [not

shown here] and L peaks at ∼2.7 keV) were observed, along with those of P (K peaks at ∼2 keV) and Ca (L peaks at ∼3.7 and ∼4.0 keV).

3.2. Alcohol oxidation

It was shown earlier [35] that RuHAp is a good and highly selective catalyst for the oxidation of aromatic and allylic alcohols to the corresponding carbonyl compounds with oxygen, but transformation of aliphatic primary and secondary alcohols was sluggish and incomplete. Hence, here the catalytic activity of the RuHAp samples was tested mainly in the oxidation of benzyl alcohol (Table 2). With the exception of RuHAp-Phos, organic modification led to considerably higher activity, and all catalysts produced only benzaldehyde with no further oxidation to benzoic acid even at high conversions. The best catalysts were prepared by method II; that is, Ru was incorporated into HAp samples synthesized in the presence of organic modifiers. On the basis of the TOF values determined at 5% (TOF_0) or full conversion (TOF_{av}), the modified catalysts outperformed the reference sample by a factor of about 2–3. The time profile of the oxidation of benzyl alcohol and 2-octanol with RuHAp and RuHAp-prolinol is shown in Fig. 4 as examples.

A preliminary kinetic study revealed that oxidation of benzyl alcohol was not free from mass transport limitations. As discussed previously [36], at relatively low temperatures the removal of water co-product from the catalyst surface was slow and rate-limiting. Application of temperatures close to the boiling point of the solvent accelerated the removal of water but decreased the oxygen partial pressure, and reoxidation of the ruthenium-hydride species in RuHAp became the rate-limiting step. Higher oxidation rates were achieved by replacing toluene with mesitylene, which has a lower vapor pressure, and by reducing the amount of solvent and catalyst (cf. Tables 2 and 3). Even with this, however, inhibition of the global reaction rate by accumulation of the co-product water could not be eliminated at conversions higher than about 5%.

The results of the oxidation of *para*-substituted benzyl alcohols are summarized in Table 3. Almost complete conversion and 100% selectivity to the corresponding aldehydes were achieved within 15–45 min, despite the moderate reaction temperature (333 K). The decelerating effect of the electron-withdrawing substituents (–NO₂, –Cl; Hammett substituent constant $\sigma > 0$) on the average TOF values can be clearly seen, but the electron-donating substituents (–OMe, –Me; $\sigma < 0$) did
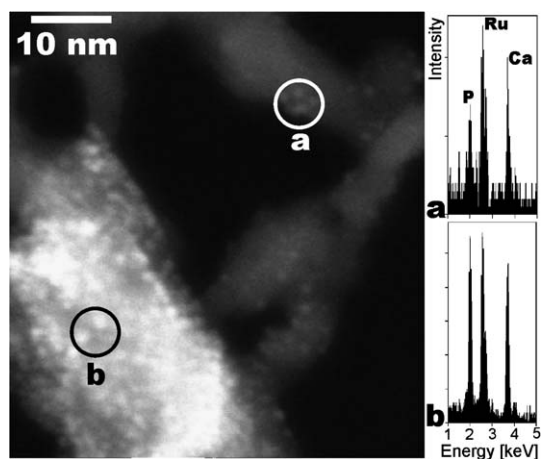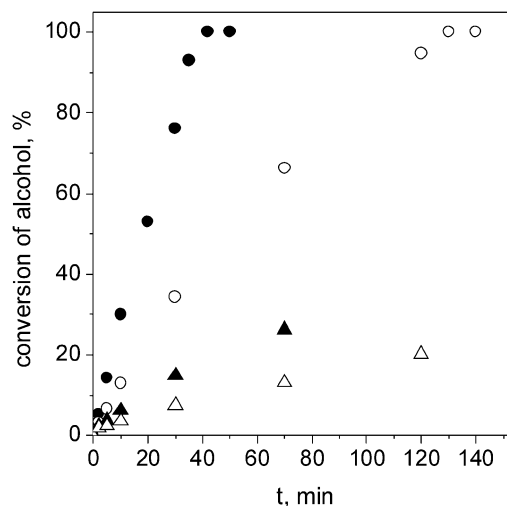

Fig. 3. HAADF-STEM image of RuHAp-BAcid and EDXS spot analyses performed at points a and b. Only a section of the EDX spectra with peaks of P, Ru and Ca is shown. The presence of Ru peaks in the spectra proves that the bright spots in the HAADF-STEM images correspond to Ru species.

Fig. 4. Oxidation of benzyl alcohol with RuHAp (○) and RuHAp-prolinol (●), oxidation of 2-octanol with RuHAp (△) and RuHAp-prolinol (▲). Reaction conditions: 60 mg catalyst, 1 mmol benzyl alcohol, 10 ml toluene, 333 K, 1 bar O₂.

Table 2
Catalytic oxidation of benzyl alcohol with molecular oxygen; the selectivity to benzaldehyde was always 100%[a]

Catalyst	Organic modification method	t (min)	Yield (%)	TOF_0 (h^{-1})	TOF_{av} (h^{-1})
RuHAp	–	130	>99	36	21
RuHAp-Phos	I	155	>99	38	23
RuHAp-HAcid	I	66	>99	74	54
RuHAp-BAcid	II	49	>99	82	66
RuHAp-proline	II	57	>99	72	50
RuHAp-prolinol	II	42	>99	78	70

[a] Reaction conditions: 60 mg catalyst, 1 mmol benzyl alcohol, 10 ml toluene, 333 K, 1 bar O₂.

Table 3
Catalytic oxidation of benzyl alcohols with molecular oxygen according to Scheme 1; the selectivity to benzaldehyde was always 100%[a]

Entry	X	m (catal.) (mg)	t (min)	Yield (%)	TOF_{av} (h^{-1})
1	H	60	15	>99	215
2	H	40	20	>99	242
3	Me	60	17	>99	190
4	MeO	60	17	>99	190
5	Cl	60	20	>99	161
6	NO₂	60	45	98	72

[a] Reaction conditions: RuHAp-BAcid, 1 mmol alcohol, 4 ml mesitylene, 333 K, 1 bar O₂.
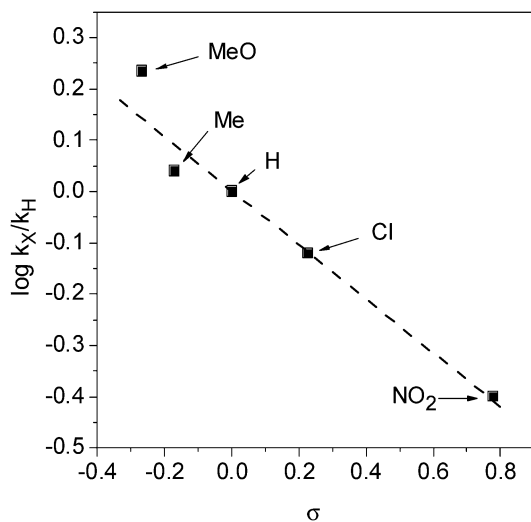
Fig. 5. Hammett plot of p-substituted benzyl alcohols. Reaction conditions: 1 mmol p-X-benzyl alcohol (X = H, Cl, NO_2, Me, or MeO), 10 mg RuHAp-BAcid (0.0031 mmol Ru), 4 ml mesitylene, 333 K, 1 bar O_2, $t = 2$ min.

not increase the rate, because of mass transport limitations in the system. Hence, the study of the effect of *para* substituents on the initial reaction rate was repeated under kinetically controlled conditions, and the k_X/k_H values were determined from conversions <5%. The Hammett plot is shown in Fig. 5. The accelerating effect of electron-donating substituents and the decelerating effect of electron-withdrawing substituents indicate that the dehydrogenation step (β-hydride elimination) is rate-limiting and the reaction is kinetically controlled [52,53]. The slope of the Hammett plot ($\rho \approx -0.54$) is similar to those slopes observed in the oxidation of benzyl alcohol with 17 wt% RuHAp ($\rho = -0.43$) [33], $RuCl_2(PPh_3)_3$ ($\rho = -0.58$ by TEMPO/Ru = 6:1) [54], and Ru/Al_2O_3 ($\rho = -0.46$) [7].

To test the stability of organically modified RuHAp, the reaction was interrupted at about 60% conversion, the catalyst was filtered off from the hot reaction mixture, and the filtrate was reacted under the reaction conditions. But even with these measures, no further conversion (i.e., no leaching of the active species leading to homogeneous catalysis) was detectable.

The possibility of repeated use of RuHAp was also tested. After full conversion of benzyl alcohol, an equal molar amount of 4-methyl-benzyl alcohol was added to the slurry, and the reaction was completed. Next, the same procedure was repeated with the opposite sequence of alcohol addition. The average reaction rates in the oxidation of benzyl alcohol were almost identical, independent of the order of addition of the two substrates. Note that in this way the loss of catalyst during filtration and recovery can be avoided.

3.3. Structure of RuHAp analyzed by DRIFT spectroscopy

To gain information on the structure of the catalysts at the molecular level, we investigated all of the catalyst samples by DRIFT spectroscopy. Some examples indicating the potential of this technique in the characterization of HAp-based catalysts are collected in Figs. 6 and 7. The DRIFT spectrum of HAp-proline (Fig. 6c) features the complete set of signals
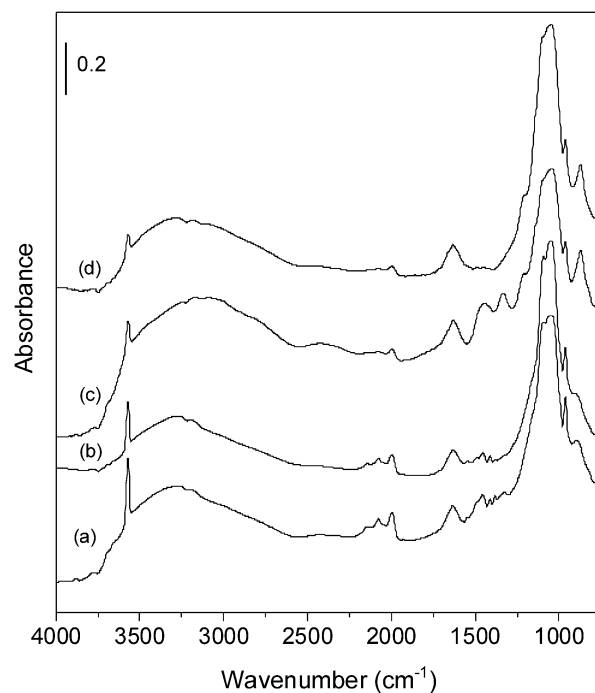

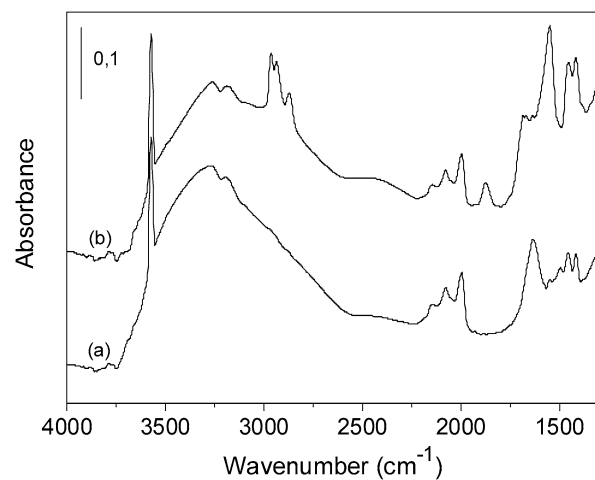Fig. 6. DRIFT spectra of (a) HAp, (b) RuHAp, (c) HAp-proline, and (d) RuHAp-proline.

Fig. 7. DRIFT spectra of RuHAp-HA prepared by Ru incorporation after organic modification with hexanoic acid (method I, curve a) and by Ru incorporation before organic modification with hexanoic acid (curve b).

characteristic of HAp [35] with some additional bands belonging to proline. HAp (Fig. 6a) produced the characteristic ν(OH) vibrations of lattice hydroxyls at 3570 cm^{-1}; asymmetric and symmetric stretch modes of PO_4^{3-} at 1093, 1043, and 962 cm^{-1}; and a set of overtone and combination bands at 2200–1950 cm^{-1}. The broad envelope extending from 3800–2500 cm^{-1}, together with the signal at ca. 1640 cm^{-1}, suggest the presence of surface water molecules. Carbonates, originating from the CO_2 adsorption from the air during sample handling [55], are identified by the set of signals in the 1700–1300 cm^{-1} spectral region.

Incorporation of proline in HAp-proline is confirmed by the signals at 1448 and 1336 cm^{-1}, assigned to the symmetric

OCO stretch and bending modes of the side chain, respectively (Fig. 6c). The attenuation of the signal at 3570 cm^{-1} and the increased broadening of the envelope at 3800–2500 cm^{-1} indicate the interaction of the carboxyl group of proline with OH functions of the HAp lattice. These changes in the signal of lattice hydroxyls and surface water were found only in the samples prepared by method II (HAp-proline, HAp-prolinol, and HAp-BA) and not in HAp-Phos and HAp-HA (spectra not shown here), which were prepared by the surface modification method (method I).

The signals corresponding to adsorbed proline disappeared after incorporation of Ru in RuHAp-proline (Fig. 6d). We observed the same phenomenon in the case of RuHAp-Phos and RuHAp-HA samples and the almost complete removal (dissolution) of benzoic acid and prolinol from HAp-BA and HAp-prolinol (not shown here). The CH absorption bands characteristic for HAp-Phos and HAp-HA at 2966, 2935, 2880, and 2866 cm^{-1}; the bands of carboxyl group in the spectra of HAp-HA and HAp-BA at 1550/1545 and 1415/1385 cm^{-1}; and the characteristic broad bands of HAp-prolinol at 1460 and 1340 cm^{-1} disappeared or diminished greatly after treatment of the organically modified HAp with aqueous acidic (pH = 2.2) RuCl$_3$ solution. Interestingly, after introduction of Ru, the signal of lattice hydroxyls, which was attenuated through the interaction with the organic modifiers proline (Fig. 6, spectra c and d), prolinol, and benzoic acid, did not change. This unexpected observation may be explained by the assumption that Ru occupies the same adsorption sites as the organic modifiers.

To confirm the leaching of organic modifier during incorporation of Ru, we prepared two catalysts by surface modification of RuHAp (instead of HAp according to method I) with 2-ethylhexyl-phosphate (RuHAp-Phos*) and hexanoic acid (RuHAp-HA*). The DRIFT spectra of these samples revealed the presence of organic modifiers, in contrast to the structure of RuHAp-Phos and RuHAp-HA, which were prepared by method I. The striking structural difference is illustrated in Fig. 7 for the example of hexanoic acid-modified RuHAp, where the presence of hexanoic acid was confirmed by the bands at 2966, 2935, 2880, and 2866 cm^{-1} [ν(C–H)] and at 1550 cm^{-1} [ν_{as}(OCO)]. The appearance of the band at 1880 cm^{-1} in hexanoic acid-modified RuHAp demonstrates the presence of ruthenium as described in our previous paper [35]. RuHAp-Phos* and RuHAp-HA* were poorly active in alcohol oxidation; the TOF$_0$ in benzyl alcohol oxidation decreased from 38 h^{-1} (RuHAp-Phos, Table 2) to 7 h^{-1} (RuHAp-Phos*), and from 74 h^{-1} (RuHAp-HA, Table 2) to 5 h^{-1} (RuHAp-HA*). Clearly, the organic modifier applied according to methods I and II influences the structure of HAp (and thus RuHAp), but it leaches out during the subsequent incorporation of Ru and does not disturb the catalytic application of the new materials.

4. Discussion

Two different methods have been used for the successful organic modification of RuHAp. In a three-step synthesis, the organic compound was added to the conventionally prepared HAp (method I), and in the two-step route the organic modifier was present already during the synthesis of HAp (method II). In both cases, Ru ions were incorporated into the organically modified HAp. An inverted approach, organic modification after introduction of Ru, proved inferior due to the poor oxidation activity of the catalysts. Method II seems to be the most promising route, because of its simplicity and the high activity of the resulting catalysts. A limitation of this route is that only water-soluble organic modifiers can be used together with Ca(NO$_3$)$_2$ and (NH$_4$)$_2$HPO$_4$ in the aqueous-phase synthesis of HAp.

Organic modification of HAp by methods I and II resulted in different morphologies of the samples (Fig. 1) and remarkably higher activity in the oxidation of benzyl alcohol and 2-octanol (Table 2; Fig. 4). An important point is that organic modification did not diminish the excellent selectivity of RuHAp to benzaldehyde (100%). The efficient modifiers include carboxylic acids (hexanoic and benzoic acids), an amino acid (proline), and an amino alcohol (prolinol). A common feature of these compounds is that they can interact strongly with the OH and phosphate functions of the HAp matrix via H bonding.

The enhanced catalytic activity may be traced to an increase in the number of accessible Ru sites and higher activity of Ru species due to differing coordination to the HAp lattice. To estimate the number of accessible active sites, the transformation of benzyl alcohol to benzaldehyde was investigated under Ar. In the absence of molecular oxygen, the active sites are rapidly reduced and become inactive in the further transformation of benzyl alcohol [36]. For these reactions, 0.2 mmol of benzyl alcohol and 50 mg of RuHAp or RuHAp-prolinol were used in 10 mL of toluene under the reaction conditions described in the Experimental section. The conversion of benzyl alcohol after 10 min leveled off at 4% with RuHAp and at 4.3% with RuHAp-prolinol. The corresponding turnover number (TON) values were 0.43 for RuHAp and 0.51 for RuHAp-prolinol. Clearly, the 19% increase in the number of accessible (reducible) sites cannot explain the more than threefold-greater catalytic activity of the organically modified catalyst (Table 2). Note that the 19% increase in the TON is smaller than the difference between the BET surface areas of RuHAp-prolinol and RuHAp (65%; Table 1).

We assume that the major reason for the enhanced activity of organically modified RuHAp is the higher intrinsic activity of the ruthenium species due to their different location and coordination. The results of the ICP-OES (Table 1) and DRIFT measurements (Figs. 6 and 7) suggest that incorporation of ruthenium in the organically modified HAp lattice occurred in a different way than the incorporation of ruthenium into HAp. The ion exchange between Ru^{3+} and Ca^{2+} in the organically modified HAp can be excluded based on the Ca/P ratios (Table 1). Note that ion exchange as the dominant mechanism of incorporating metal ions into HAp has already come under question [56–59]. The DRIFT measurements revealed similar coordination in the ruthenium species and the organic modifiers to the lattice hydroxyl groups. It is very probable that in organically modified HAp, ruthenium is located mainly on the outer surface and anchored to phosphate and hydroxyl groups. These sites are more accessible to the relatively bulky alcohol

Table 4
Comparison of highly selective catalysts in the oxidation of benzyl alcohol to benzaldehyde with oxygen

Catalyst	T (K)	$p(O_2)$ (bar)	Solvent	Conversion (%)	Yield (%)	TOF$_{av}$ (h^{-1})	Reference
Ru$^{(III)}$/HAp	353	1	PhCH$_3$	100	>99	2	[33]
Ru$^{(III)}$Co$^{(II)}$/HAp	363	1	PhCH$_3$	100	>99	78	[35]
Ru$^{(III)}$/HAp-BAcid	333	1	Mesitylene	100	>99	242	Present work
Ru$^{(IV)}$Mn$^{(IV)}$Mn$^{(IV)}$/HT	333	1	PhCH$_3$	100	99	50	[11]
Ru$^{(IV)}$Co$^{(III)}$/Al$_2$O$_3$	383	1	PhCH$_3$	100	>99	80	[12]
Ru$^{(III)}$/TiO$_2$ nanotube	390	8	PhCH$_3$	75	75	450	[13]
Ru$^{(III)}$/TiO$_2$	353	4	C$_6$H$_4$Cl$_2$	100	100	100	[14]
Pd/HAp	363	1	PhCF$_3$	>99	99	500	[17]
Pd/Al(OH)$_3$	343	1	PhCH$_3$	–	>99	100	[60]

substrate, and thus the transport processes are enhanced in the catalyst particle.

In the oxidation of benzyl alcohol over RuHAp modified with benzoic acid (RuHAp-BAcid), TOFs up to 242 h^{-1} (Table 3) could be achieved at full conversion with no further oxidation of benzaldehyde to benzoic acid. The reaction was complete in 20 min under very mild conditions (333 K, 1 bar). The activity is about threefold higher than that of the cobalt-promoted RuHAp [35] and more than two orders of magnitude greater than that of the original RuHAp catalyst [33], as shown in Table 4. When considering the different reaction temperatures, the development is even more impressive.

Characteristic data of other catalysts that afford at least 99% chemoselectivity and high average rates at high conversion in the aerobic oxidation of benzyl alcohol to benzaldehyde are collected in Table 4. The highest rates (TOF = 450–500 h^{-1}) were reported for Pd supported on HAp [17] and hydrated ruthenium oxide supported on titania nanotubes [13]. When considering the more forcing reaction conditions (higher temperature, partially higher pressure), the activity of our catalyst seems comparable with the two best examples.

5. Conclusion

Ruthenium-exchanged hydroxyapatite is a promising new catalyst for various oxidation reactions using molecular oxygen as the sole source of oxidant. Our working hypothesis was that the catalyst activity can be improved by fine-tuning the structure of the catalyst, including the location and accessibility of the Ru active sites. The first successful example of this approach has been published recently [35]. Here we presented a new methodology, involving modification of the host material by adding polar organic compounds able to form strong hydrogen bonds with the OH and phosphate functions of hydroxyapatite. ICP-OES, N$_2$ adsorption, SEM, and DRIFT spectroscopy revealed that the twofold-to-threefold greater activity of ruthenium-hydroxyapatite modified by hexanoic acid, benzoic acid, prolinol, or proline is due mainly to different location and coordination and better accessibility of the active sites, and partly to morphological changes of the apatite structure. It seems that the organic modifiers act as "templating agents" for the controlled location and coordination of the Ru species, but they leach out during incorporation of Ru and thus do not bias the catalytic process. In other words, the strikingly different chemical compounds act as structural modifiers but are (practically) absent in the final RuHAp catalyst. If the modifiers are added to the catalyst after the incorporation of Ru, they diminish the oxidation activity dramatically.

References

[1] R.A. Sheldon, H. van Bekkum, Fine Chemicals through Heterogeneous Catalysis, Wiley–VCH, Weinheim, 2001, p. 473.
[2] M. Besson, P. Gallezot, Catal. Today 57 (2000) 127.
[3] B.M. Choudary, M.L. Kantam, P.L. Santhi, Catal. Today 57 (2000) 17.
[4] I.W.C.E. Arends, R.A. Sheldon, in: E. Bäckvall (Ed.), Modern Oxidation Methods, Wiley–VCH, Weinheim, 2004, p. 83.
[5] B.Z. Zhan, A. Thompson, Tetrahedron 60 (2004) 2917.
[6] T. Mallat, A. Baiker, Chem. Rev. 104 (2004) 3037.
[7] K. Yamaguchi, N. Mizuno, Chem.-Eur. J. 9 (2003) 4353.
[8] B.Z. Zhan, M.A. White, T.K. Sham, J.A. Pincock, R.J. Doucet, K.V.R. Rao, K.N. Robertson, T.S. Cameron, J. Am. Chem. Soc. 125 (2003) 2195.
[9] K. Ebitani, H.B. Ji, T. Mizugaki, K. Kaneda, J. Mol. Catal. A 212 (2004) 161.
[10] T. Matsushita, K. Ebitani, K. Kaneda, Chem. Commun. (1999) 265.
[11] K. Ebitani, K. Motokura, T. Mizugaki, K. Kaneda, Angew. Chem., Int. Ed. 44 (2005) 3423.
[12] T.L. Stuchinskaya, M. Musawir, E.F. Kozhevnikova, I.V. Kozhevnikov, J. Catal. 231 (2005) 41.
[13] D.V. Bavykin, A.A. Lapkin, P.K. Plucinski, J.M. Friedrich, F.C. Walsh, J. Catal. 235 (2005) 10.
[14] A. Köckritz, M. Sebek, A. Dittmar, J. Radnik, A. Brückner, U. Bentrup, M.-M. Pohl, H. Hugl, W. Mägerlein, J. Mol. Catal. A: Chem. 246 (2006) 85.
[15] T. Mallat, A. Baiker, Catal. Today 19 (1994) 247.
[16] P. Gallezot, Catal. Today 37 (1997) 405.
[17] K. Mori, K. Yamaguchi, T. Hara, T. Mizugaki, K. Ebitani, K. Kaneda, J. Am. Chem. Soc. 124 (2002) 11572.
[18] S. Biella, G.L. Castiglioni, C. Fumagalli, L. Prati, M. Rossi, Catal. Today 72 (2002) 43.
[19] L. Prati, F. Porta, Appl. Catal. A 291 (2005) 199.
[20] S. Carrettin, P. McMorn, P. Johnston, K. Griffin, C.J. Kiely, G.A. Attard, G.J. Hutchings, Top. Catal. 27 (2004) 131.
[21] A. Abad, P. Concepcion, A. Corma, H. Garcia, Angew. Chem., Int. Ed. 44 (2005) 4066.
[22] D.I. Enache, J.K. Edwards, P. Landon, B. Solsona-Espriu, A.F. Carley, A.A. Herzing, M. Watanabe, C.J. Kiely, D.W. Knight, G.J. Hutchings, Science 311 (2006) 362.
[23] V.R. Choudhary, A. Dhar, P. Jana, R. Jha, B.S. Uphade, Green Chem. 7 (2005) 768.
[24] D.I. Enache, D.W. Knight, G.J. Hutchings, Catal. Lett. 103 (2005) 43.
[25] S. Sebti, A. Solhy, R. Tahir, A. Smahi, Appl. Catal. A 235 (2002) 273.
[26] R. Tahir, K. Banert, S. Sebti, Appl. Catal. A 298 (2006) 261.

[27] F. Bazi, H. El Badaoui, S. Tamani, S. Sokori, A. Solhy, D.J. Macquarrie, S. Sebti, Appl. Catal. A 301 (2006) 211.
[28] S. Sebti, R. Tahir, R. Nazih, A. Saber, S. Boulaajaj, Appl. Catal. A 228 (2002) 155.
[29] A. Smahi, A. Solhy, H. El Badaoui, A. Amoukal, A. Tikad, M. Maizi, S. Sebti, Appl. Catal. A 250 (2003) 151.
[30] S. Sebti, R. Tahir, R. Nazih, S. Boulaajaj, Appl. Catal. A 218 (2001) 25.
[31] M. Zahouily, Y. Abrouki, B. Bahlaouan, A. Rayadh, S. Sebti, Catal. Commun. 4 (2003) 521.
[32] Y. Maeda, Y. Washitake, T. Nishimura, K. Iwai, T. Yamauchi, S. Uemura, Tetrahedron 60 (2004) 9031.
[33] K. Yamaguchi, K. Mori, T. Mizugaki, K. Ebitani, K. Kaneda, J. Am. Chem. Soc. 122 (2000) 7144.
[34] S. Wuyts, D.E. De Vos, F. Verpoort, D. Depla, R. De Gryse, P.A. Jacobs, J. Catal. 219 (2003) 417.
[35] Z. Opre, J.D. Grunwaldt, M. Maciejewski, D. Ferri, T. Mallat, A. Baiker, J. Catal. 230 (2005) 406.
[36] Z. Opre, J.D. Grunwaldt, T. Mallat, A. Baiker, J. Mol. Catal. A: Chem. 242 (2005) 224.
[37] H. Tanaka, A. Yasukawa, K. Kandori, T. Ishikawa, Langmuir 13 (1997) 821.
[38] T. Ishikawa, H. Tanaka, A. Yasukawa, K. Kandori, J. Mater. Chem. 5 (1995) 1963.
[39] H. Tanaka, A. Yasukawa, K. Kandori, T. Ishikawa, Colloids Surf. A 125 (1997) 53.
[40] H. Tanaka, T. Watanabe, M. Chikazawa, K. Kandori, T. Ishikawa, Colloids Surf. A 139 (1998) 341.
[41] L. Borum-Nicholas, O.C. Wilson, Biomaterials 24 (2003) 3671.
[42] H. Tanaka, T. Watanabe, M. Chikazawa, K. Kandori, T. Ishikawa, J. Colloid Interface Sci. 214 (1999) 31.
[43] G.M.S. El Shafei, N.A. Moussa, J. Colloid Interface Sci. 238 (2001) 160.
[44] T. Matsumoto, M. Okazaki, M. Inoue, Y. Hamada, M. Taira, J. Takahashi, Biomaterials 23 (2002) 2241.
[45] S. Koutsopoulos, E. Dalas, Langmuir 16 (2000) 6739.
[46] R. Gonzalez-McQuire, J.Y. Chane-Ching, E. Vignaud, A. Lebugle, S. Mann, J. Mater. Chem. 14 (2004) 2277.
[47] G.V. Rodicheva, V.P. Orlovskii, N.M. Romanova, Russ. J. Inorg. Chem. 45 (2000) 1819.
[48] N. Spanos, P.G. Koutsoukos, Langmuir 17 (2001) 866.
[49] S. Sugiyama, T. Minami, H. Hayashi, M. Tanaka, N. Shigemoto, J.B. Moffat, J. Chem. Soc., Faraday Trans. 92 (1996) 293.
[50] S.J. Pennycook, Ultramicroscopy 30 (1989) 58.
[51] J. Liu, Microsc. Microanal. 10 (2004) 55.
[52] J.A. Mueller, C.P. Goller, M.S. Sigman, J. Am. Chem. Soc. 126 (2004) 9724.
[53] K.A. Connors, Chemical Kinetics, The Study of Reaction Rates in Solution, VCH, New York, 1990.
[54] A. Dijksman, A. Marino-Gonzalez, A.M.I. Payeras, I. Arends, R.A. Sheldon, J. Am. Chem. Soc. 123 (2001) 6826.
[55] Z.H. Cheng, A. Yasukawa, K. Kandori, T. Ishikawa, J. Chem. Soc., Faraday Trans. 94 (1998) 1501.
[56] Y.P. Xu, F.W. Schwartz, S.J. Traina, Environ. Sci. Technol. 28 (1994) 1472.
[57] M. Wakamura, K. Kandori, T. Ishikawa, Colloids Surf. A 142 (1998) 107.
[58] Q.Y. Ma, S.J. Traina, T.J. Logan, J.A. Ryan, Environ. Sci. Technol. 27 (1993) 1803.
[59] A. Crosman, G. Gelbard, G. Poncelet, V.I. Parvulescu, Appl. Catal. A 264 (2004) 23.
[60] M.S. Kwon, N. Kim, C.M. Park, J.S. Lee, K.Y. Kang, J. Park, Org. Lett. 7 (2005) 1077.